DOI: 10.19884/j.1672-5220.202410004

Preparation and Power Frequency Shielding Effectiveness of Stainless Steel Conductive Fabric

YANG Yang[1], ZHANG Yan[1], ZHANG Ruiyun[1*], JI Feng[1], LI Wenjun[2], XU Xiaoyuan[3]
1. College of Textiles, Donghua University, Shanghai 201620, China
2. Hangzhou Segurmax Textile Co., Ltd., Hangzhou 311215, China
3. China Cotton Textile Association, Beijing 100027, China

Abstract: In order to prepare the shielding fabrics with high efficiency of power frequency (PF) shielding and excellent electrical conductivity, different ratios of aramid/stainless steel fiber blended yarns were used to weave the shielding fabrics with different specifications. The fabric structure, fabric areal density, number of fabric layers, embedding ratio of copper-clad wires wrapped aramid yarns (denoted as CCWWA) and embedding direction were designed, and a total of 34 different types of shielding fabrics were woven for testing. The experiments were mainly conducted to study the influence mechanism of various factors on the PF shielding effectiveness by testing the electrical conductivity and PF shielding effectiveness of the fabrics. The research results indicate that the PF shielding effectiveness improves with increasing fabric areal density and metal fiber content. The fabrics embedded with CCWWA, particularly those with bidirectional embedding, exhibit a significant enhancement in the PF shielding effectiveness, showing an increase of 8 – 20 dB compared to the fabrics without CCWWA. The PF shielding effectiveness varies across different fabric structures, with plain weave fabrics demonstrating the superior PF shielding effectiveness due to their compact structure. Non-conductive base fabric has minimal impact on the PF shielding effectiveness. As the number of fabric layers increases, the PF shielding effectiveness initially improves but then declines, peaking with double-layer fabrics.

Keywords: stainless steel blended fabric; power frequency; shielding effectiveness; conductivity; safety protection
CLC number: TS101.923 **Document code**: A
Article ID: 1672-5220(2025)05-0476-09

Open Science Identity (OSID)

0 Introduction

In the highly informatized modern society, electromagnetic waves have extensively permeated various domains of human life[1-2]. Electronic devices in daily life and working environments generate electromagnetic waves across different frequency bands[3-4]. High-frequency electromagnetic waves are primarily emitted by communication equipment, microwave ovens, radar systems and medical devices. Their radiation poses health hazards to humans and causes interference with electronic devices. In the low-frequency electromagnetic spectrum, the most typical interference band is the power frequency (PF) band (50 Hz), mainly generated by industrial and household electricity. Notably, long-term exposure to high-voltage PF electromagnetic environments may induce occupational diseases such as neurophysiological disorders and cardiovascular system abnormalities[5-9].

In the field of shielding materials, composite films exhibit excellent electromagnetic wave absorption properties, yet they suffer from poor wear comfort and are predominantly applied to high-frequency protection. Conversely, textile-based materials demonstrate favorable wearability but lack sufficient protective performance. To meet long-term wearing requirements, conventional shielding garments predominantly utilize textile-based materials. Consequently, existing protective clothing for high-voltage live-line workers generally provides only basic shielding performance, failing to satisfy the increasingly stringent shielding demands imposed by growing signal transmission intensities.

To address the inadequate PF shielding performance of current protective clothing, this study designs PF shielding fabrics by adjusting yarn types and fabric structural parameters. Through the resistance and the PF shielding effectiveness testing of woven samples, the electrical conductivity and the PF shielding effectiveness of the fabrics with different specifications are comparatively analyzed, providing a reference basis for designing highly conductive and high-performance shielding protective clothing.

1 Materials and Methods

1.1 Materials

The specifications of the yarns used in the

Received date: 2024-10-16
Foundation item: Taishan Industrial Experts Program, China
* Correspondence should be addressed to ZHANG Ruiyun, email: ryzhang@dhu.edu.cn
Citation: YANG Y, ZHANG Y, ZHANG R Y, et al. Preparation and power frequency shielding effectiveness of stainless steel conductive fabric [J]. *Journal of Donghua University (English Edition)*, 2025, 42(5): 476-484.

experiment are shown in Table 1. Samples #1 to #4 are blended yarns; sample #5 is a single compositon yarn; sample #6 is a covered yarn.

Table 1 Specifications of yarns

No.	Yarn name	Yarn specification
#1	SS/PMIA/FRV(30/40/30)	36S/2
#2	SS/PMIA(40/60)	30S/2
#3	SS/T(30/70)	36S/2
#4	SS/PMIA(20/80)	36S/2
#5	PMIA	35S/2
#6	CCWWA	200D+35S/1

Notes: SS denotes stainless steel fiber; PMIA represents Nomex yarn; FRV stands for flame retardant viscose fiber; T indicates Tencel fiber; the numbers in parentheses indicate the mass ratio of fibers in the blend; CCWWA is the copper-clad wire-wrapped aramid yarn; D refers to Denier, a fixed-length unit of yarn fineness, while S refers to the English cotton count, a fixed-weight unit of yarn fineness; /1 and /2 indicate that the yarn is made from one and two strands, respectively.

1.2 Fabric preparation

Different blended yarns were selected to weave four types of blended fabrics on an automatic rapier loom. The fabric weave structures were plain and basket. Fabrics with varying metal contents, different metal fiber types, distinct arrangements and diverse woven structures were selected as the raw materials for the experiments. The specifications of the fabrics are detailed in Table 2, and a total of six comparative experiments were designed to analyze the influencing factors. The fabrics are categorized into four classes: A, B, C and D (Table 2). A total of 34 fabrics were designed, with two types of yarns selected for the warp: PMIA and CCWWA yarns. The weft yarns included SS/PMIA/FRV (30/40/30) blended yarn, SS/PMIA (40/60) blended yarn, SS/T (30/70) blended yarn, SS/PMIA (20/80) blended yarn, PMIA yarn and CCWWA covered yarn. The fabric weave structures were plain and basket, and the warp yarn density was set at 20 ends/cm.

Table 2 Fabric parameters

Fabric No.	Warp yarn 1	Warp yarn 2	Warp rod ratio	Weft yarn 1	Weft yarn 2	Weft rod ratio	Warp density/(ends/cm)	Weft density/(picks/cm)	Fabric weave structure
A1	PMIA	PMIA	—	SS/PMIA/FRV (30/40/30)	SS/PMIA/FRV (30/40/30)	—	20	20	Plain
A2	PMIA	PMIA	—	SS/PMIA/FRV (30/40/30)	SS/PMIA/FRV (30/40/30)	—	20	15	Plain
A3	PMIA	PMIA	—	SS/PMIA/FRV (30/40/30)	SS/PMIA/FRV (30/40/30)	—	20	10	Plain
A4	PMIA	PMIA	—	SS/PMIA/FRV (30/40/30)	PMIA	1:1	20	25	Plain
A5	PMIA	PMIA	—	SS/PMIA/FRV (30/40/30)	PMIA	1:1	20	20	Plain
A6	PMIA	PMIA	—	SS/PMIA/FRV (30/40/30)	CCWWA	5:1	20	20	Plain
A7	PMIA	PMIA	—	SS/PMIA/FRV (30/40/30)	CCWWA	9:1	20	20	Plain
A8	PMIA	PMIA	—	SS/PMIA/FRV (30/40/30)	CCWWA	15:1	20	20	Plain
A9	PMIA	PMIA	—	SS/PMIA/FRV (30/40/30)	CCWWA	19:1	20	20	Plain
A10	PMIA	PMIA	—	SS/PMIA/FRV (30/40/30)	CCWWA	15:1	20	20	Basket
A11	PMIA	CCWWA	15:1	SS/PMIA/FRV (30/40/30)	CCWWA	15:1	20	20	Plain
A12	PMIA	CCWWA	15:1	SS/PMIA/FRV (30/40/30)	CCWWA	15:1	20	20	Basket
A13	PMIA	PMIA	—	SS/PMIA/FRV (30/40/30)	CCWWA	19:1	20	20	Plain
A14	PMIA	PMIA	—	SS/PMIA/FRV (30/40/30)	CCWWA	38:2	20	20	Plain
A15	PMIA	PMIA	—	SS/PMIA/FRV (30/40/30)	CCWWA	57:3	20	20	Plain

(Table 2 continued)

Fabric No.	Warp yarn 1	Warp yarn 2	Warp rod ratio	Weft yarn 1	Weft yarn 2	Weft rod ratio	Warp density/ (ends/cm)	Weft density/ (picks/cm)	Fabric weave structure
B1	PMIA	PMIA	—	SS/PMIA(40/60)	SS/PMIA(40/60)	—	20	20	Plain
B2	PMIA	PMIA	—	SS/PMIA(40/60)	SS/PMIA(40/60)	—	20	15	Plain
B3	PMIA	PMIA	—	SS/PMIA(40/60)	SS/PMIA(40/60)	—	20	10	Plain
B4	PMIA	PMIA	—	SS/PMIA(40/60)	CCWWA	15∶1	20	20	Plain
B5	PMIA	PMIA	—	SS/PMIA(40/60)	CCWWA	15∶1	20	20	Basket
B6	PMIA	CCWWA	15∶1	SS/PMIA(40/60)	CCWWA	15∶1	20	20	Plain
B7	PMIA	CCWWA	15∶1	SS/PMIA(40/60)	CCWWA	15∶1	20	20	Basket
C1	PMIA	PMIA	—	SS/T(30/70)	SS/T(30/70)	—	20	30	Plain
C2	PMIA	PMIA	—	SS/T(30/70)	SS/T(30/70)	—	20	27	Plain
C3	PMIA	PMIA	—	SS/T(30/70)	SS/T(30/70)	—	20	20	Plain
C4	PMIA	PMIA	—	SS/T(30/70)	CCWWA	15∶1	20	20	Plain
C5	PMIA	PMIA	—	SS/T(30/70)	CCWWA	15∶1	20	20	Basket
C6	PMIA	CCWWA	15∶1	SS/T(30/70)	CCWWA	15∶1	20	20	Plain
C7	PMIA	CCWWA	15∶1	SS/T(30/70)	CCWWA	15∶1	20	20	Basket
D1	PMIA	PMIA	—	SS/PMIA(20/80)	SS/PMIA(20/80)	—	20	30	Plain
D2	PMIA	PMIA	—	SS/PMIA(20/80)	SS/PMIA(20/80)	—	20	27	Plain
D3	PMIA	PMIA	—	SS/PMIA(20/80)	SS/PMIA(20/80)	—	20	20	Plain
D4	PMIA	PMIA	—	SS/PMIA(20/80)	SS/PMIA(20/80)	—	20	17	Plain
D5	PMIA	PMIA	—	SS/PMIA(20/80)	SS/PMIA(20/80)	—	20	15	Plain

Notes: warp rod ratio means the rod ratio of warp yarn 1 to warp yarn 2; weft rod ratio means the rod ratio of weft yarn 1 to weft yarn 2.

1.3 Testing and characterization

1.3.1 Fabric resistance

According to the GB/T 6568—2024 standard, the ring-shaped brass electrodes and a pressurized weight block were used to measure the point-to-point resistance value of fabric specimens. The effective test area of the ring-shaped electrode had an inner diameter of 44 mm and an outer diameter of 144 mm. The test specimen size was 240 mm × 240 mm, and it was cut at least 50 mm away from the fabric edge to avoid edge effects. The pressurized weight block was assembled in a specific sequence to ensure accurate and consistent measurements.

1.3.2 Fabric PF shielding effectiveness

The PF shielding effectiveness (hereinafter referred to as shielding effectiveness) of the fabric was measured according to the GB/T 6568—2024 standard. A voltage generator, brass electrodes, a voltmeter, a rubber plate, a brass plate and an insulating plate were assembled in the specified order. A root mean square (RMS) voltage of 600 V at a frequency of 50 Hz between the electrodes of the measuring device was applied. Following the test procedure, the reference voltage U_0 (without the test specimen) and the output voltage U_1 (with the test specimen) were recorded. The test specimen size was 180 mm × 180 mm, and its was cut at least 50 mm away from the fabric edge. The shielding effectiveness S_E was calculated by using Eq. (1), with the unit expressed in dB[10-14].

$$S_E = 20 \lg(U_0/U_1). \quad (1)$$

2 Results and Discussion

2.1 Fabric electrical conductivity

Based on the principle of the intrinsic property correlation of electromagnetic shielding materials[15-17], the resistance is a key factor to reflect the electrical conductivity (hereinafter referred to as conductivity) of fabrics. The lower the resistance, the higher the conductivity. The experimental data shown in Table 3 indicate that the higher the proportion of stainless steel fibers in the yarn, the higher the conductivity. Class B fabrics, with a stainless steel fiber content of 40%, have the higher conductivity among the four types of fabrics. In Class A fabrics, the weft rod ratios of A6, A7, A8 and A9 are 5∶1, 9∶1, 15∶1 and 19∶1, respectively; A6 has the highest conductivity and A9 has the lowest. This indicates that when the yarn fiber load and fabric structure are the same, the higher the weft rod ratio of the fabric, the lower its conductivity. Compared with A1, the resistance value of A3 increases by about 18 Ω, which means that when the yarn fiber load and fabric weave structure are the same, the tighter the structure of the fabric, the higher its conductivity. The fabric structures of A8 and A10 are plain weave and basket weave, respectively, with resistance values of 1.72 Ω and 1.93 Ω, respectively. It can be seen that, with other factors being the same, the conductivity of the plain fabric is higher than that of the basket fabric. The reasons for these differences are, on the one hand, the increased load of metal fibers in the fabric forms more continuous conductive networks, and on the other hand, the increased density of yarn interweaving points in the fabric leads to a decrease in contact resistance.

Table 3 PF shielding performance of fabrics

Fabric No.	Shielding effectiveness/dB	Resistance/Ω
A1	62.11	30.97
A2	57.05	36.91
A3	47.80	49.21
A4	63.02	36.37
A5	55.50	32.27
A6	75.53	0.97
A7	70.18	1.15
A8	68.55	1.72
A9	65.76	2.53
A10	65.42	1.93
A11	87.18	0.41
A12	81.37	0.83
A13	62.02	34.27
A14	64.84	25.67
A15	69.17	13.93
B1	83.35	1.61
B2	80.27	3.09
B3	67.80	12.55
B4	87.85	0.49
B5	85.18	1.28
B6	90.74	0.17
B7	87.86	0.56
C1	58.80	20.37
C2	54.23	24.33
C3	52.78	27.13
C4	74.54	0.89
C5	68.91	1.54
C6	87.02	0.34
C7	83.00	0.76
D1	57.11	59.71
D2	54.97	36.67
D3	49.27	33.73
D4	50.37	32.71
D5	47.38	27.33

2.2 Fabric shielding effectiveness

The conductivity of the material is one of the most important factors affecting the shielding effectiveness of fabrics[18-20]. The resistance values of the woven fabrics and their corresponding shielding effectiveness are presented in Table 3. A higher shielding effectiveness value indicates better shielding performance. For high-voltage shielding clothing used in electrical work, the Chinese national standard specifies that the shielding effectiveness value must exceed 40 dB.

Figure 1(a) is a diagram of a plain fabric structure. A grid-based analysis (Figs. 1(b) and 1(c)) is used to study the current transmission characteristics of the induced electric field under the action of a vertically incident plane wave. When metal fibers are distributed in both the warp and weft directions of the fabric, the fabric structure can be regarded as a periodic grid system composed of conductive yarns (as shown in Fig. 1(c)). This grid structure can be decomposed into two mutually orthogonal parallel periodic arrays: one parallel array system composed of warp metal yarns and the other parallel array system composed of weft metal yarns. Due to electromagnetic coupling effects, the contact impedance between adjacent conductive yarns can be neglected. Figure 1(d) shows the equivalent circuit model of the unit grid for a fabric woven with the same metal yarns in both the warp and weft directions, while Fig. 1(e) presents the equivalent circuit model for a fabric woven with two different metal yarns in the weft direction. In these equivalent circuits, the resistance R represents the contact resistance between warp and weft yarns, and the capacitance C represents the distributed capacitance generated between parallel conductors[21-22]. In Fig. 1(e), R' represents the resistance different from R.

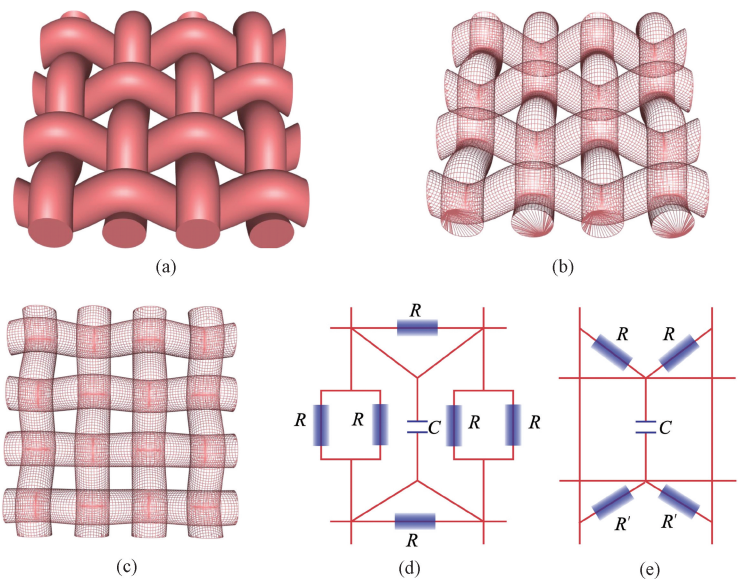

Fig. 1 Equivalent circuit of conductive shielding fabric unit: (a) diagram of plain fabric structure; (b) three-dimensional grid-based analysis diagram of plain fabric; (c) top view of Fig. 1(b); (d) equivalent circuit model for a fabric woven with the same metal yarns in both warp and weft directions; (e) equivalent circuit model for a fabric woven with two different metal yarns in weft direction

2.2.1 Influence of metal fiber content and fabric areal density on shielding effectiveness

The metal-blended yarns with varying metal fiber contents were used to investigate the effect of metal fiber content on shielding effectiveness. Additionally, the weft density of the fabrics was controlled to analyze the impact of fabric areal density on shielding effectiveness. By controlling the weft density and the type of metal-blended yarns, the effects of these two variables on the shielding effectiveness were analyzed.

Figure 2(a) shows that the shielding effectiveness of Class B fabrics is consistently higher than that of Class A fabrics, with a difference exceeding 20 dB. This is because the weft yarns in Class B fabrics contain 40% (mass fraction) stainless steel fibers, whereas those in Class A fabrics contain only 30% (mass fraction). A higher metal fiber content improves the conductive network, and enhances the conductivity of the fabric, resulting in higher shielding effectiveness.

Figure 2 shows that as the weft density increases, the shielding effectiveness of the fabric also increases. When the weft density increases from 10 to 20 picks/cm, the shielding effectiveness rises by approximately 15 dB (Fig. 2(a)). For class C and D fabrics, when the weft density increases from 20 to 30 picks/cm, the shielding effectiveness also increases, but the impact of weft density on shielding effectiveness diminishes. This is primarily because the increase in weft density raises the metal fiber content per unit area, improving the conductivity. As a result, more current is grounded through the fabric, leading to a reduction in the output voltage and an increase in shielding effectiveness. In the experiment, the fabric areal density was adjusted by altering the weft density. Overall, the shielding effectiveness of the fabrics increased gradually with the higher weft density, indicating a positive correlation between fabric areal density and shielding effectiveness. When the metal fiber content is low, the conductive network exhibits poor conductivity, resulting in inferior shielding effectiveness. As the metal fiber content increases, the metal fibers come into closer contact, forming more effective conductive pathways, which significantly enhances the shielding effectiveness.

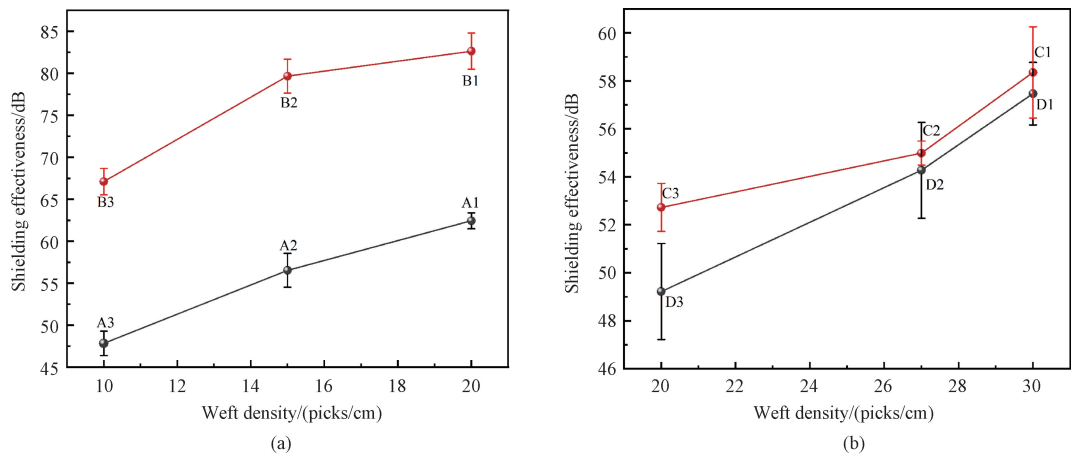

Fig. 2 Curves of shielding effectiveness vs. weft density for fabrics with different metal fiber contents: (a) Class A and B fabrics; (b) Class C and D fabrics

2.2.2 Influence of embedding direction of CCWWA on shielding effectiveness

Three sets of samples, each set with identical fabric structures but varying proportions of stainless steel fiber in the yarns, were selected from the designed samples for shielding effectiveness analysis. These three sets of samples include A1, B1 and C1 without CCWWA; A8, B4 and C4 with CCWWA embedded in the weft direction; A11, B6 and C6 with CCWWA embedded in both the warp and weft directions. Figure 3 shows that B6, with bidirectionally embedded CCWWA, exhibits the best shielding effect, with a shielding effectiveness as high as 90 dB, representing an approximately 8 dB improvement compared to B1 without CCWWA. When CCWWA are bidirectionally embedded, highly conductive yarns form a highly conductive grid pathway within the fabric, facilitating rapid current flow. In contrast, unidirectional embedding CCWWA creates a low-conductivity grid. The current flows through it resulting in a low shielding effectiveness. For fabrics without CCWWA, the current flows through a much lower-conductivity grid, resulting in slower current flow and lower conductivity. Therefore, samples A1, B1 and C1 without CCWWA exhibit the lowest shielding effectiveness among their class.

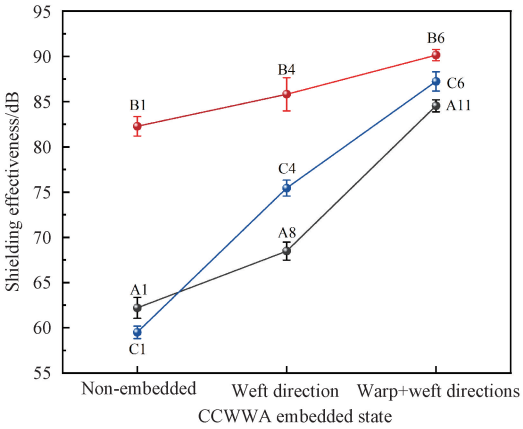

Fig. 3 Shielding effectiveness of fabrics with different CCWWA embedded states

2.2.3 Influence of proportion of CCWWA embedded in weft direction on shielding effectiveness

When the fabric structural pattern remains unchanged and CCWWA are embedded in the weft direction, its shielding effectiveness follows these rules: the greater the number of CCWWA embedded per unit area, the higher the shielding effectiveness; and when the number of CCWWA embedded per unit area is the same, the more wires embedded in the weft direction, the better the shielding performance. As shown in Fig. 4 (a), the shielding effectiveness value of A6 is the highest, and about 13 dB higher than that of A1. The reason is that the current in a circuit prefers to flow through low-resistance paths. Given that copper fibers have better conductivity than stainless steel fibers, A1, which has no embedded CCWWA, has the lowest conductivity and the lowest shielding effectiveness. As the number of embedded CCWWA increases, the number of highly conductive pathways in the weft direction of the fabric increases, improving current flow and enhancing conductivity, and thus strengthens the fabric's shielding effectiveness. A13, A14 and A15 have the same number of CCWWA embedded per unit area, with weft rod ratios of 19 : 1, 38 : 2 and 57 : 3, respectively. The analysis of their shielding effectiveness (Fig. 4 (b)) shows that the shielding effectiveness of the three-wire parallel sample A15 is about 7 dB higher than that of the single-wire distributed sample A13. According to Holm's contact theory, increasing the number of parallel-embedded conductive yarns can reduce the fabric's equivalent resistance and improve the conductivity of the equivalent circuit. For circuits formed by only one highly conductive yarn, issues such as uneven current density distribution and poor conductivity exist, which can affect the fabric's conductivity and, consequently, its shielding effectiveness.

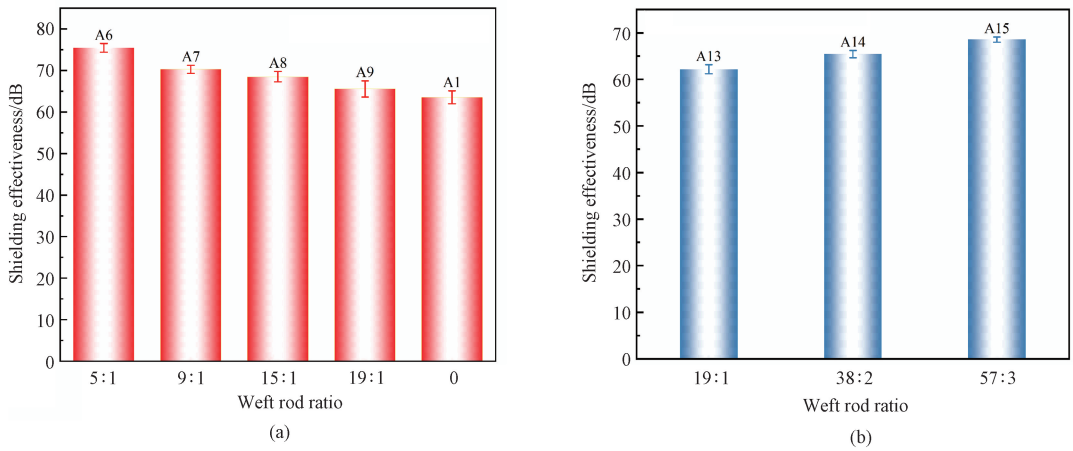

Fig. 4 Shielding effectiveness of fabrics with different weft rod ratios: (a) different number of CCWWA embedded per unit area; (b) same number of CCWWA embedded fabric per unit area

2.2.4 Influence of fabric weave structure on shielding effectiveness

For fabrics in Class A, B and C with the same organizational structure, the shielding effectiveness increases with the rise in stainless steel fiber content. Compared to unidirectional embedding at the same embedding ratio, bidirectional embedding results in an overall improvement in shielding effectiveness. Additionally, for fabrics with different organizational structures, the shielding effectiveness of plain weave fabric is higher than that of basket weave fabric (Fig. 5). This can be attributed to two main factors: yarn interweaving tightness and structure stability. Tight interweaving increases contact pressure between yarns, leading to better contact and more contact points. Fabrics with higher interweaving tightness exhibit superior shielding effectiveness. The compression during yarn interweaving causes deformation of the inter-yarn apertures, which affects the conductivity of the conductive grid. A more stable fabric structure enhances conductivity and,

consequently, shielding effectiveness.

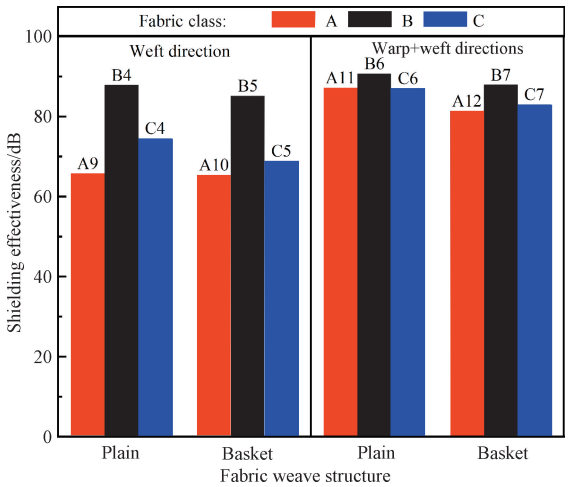

Fig. 5 Shielding effectiveness of fabrics with embedded CCWWA in different fabric weave structures

Plain weaves are the most compact, with the shortest floating length and excellent dimensional stability, resulting in a good shielding performance. In contrast, basket weaves involve two closely interwoven layers, which create non-uniform pore spaces. Under yarn compression, the conductivity of the grid in basket fabrics deteriorates, leading to inferior shielding effectiveness compared to plain weaves.

2.2.5 Influence of base fabric on shielding effectiveness

In the fabric design, A6, A7 and A8 are selected as the surface fabrics, with a pure aramid fabric used as the base fabric. The shielding effectiveness is tested, and the results are shown in Fig. 6. The differences in shielding effectiveness of the surface fabrics with and without the base fabric were not significant. Since the pure aramid fabric is non-conductive, it does not significantly affect shielding effectiveness. The shielding performance is primarily determined by the surface fabrics (A6, A7 and A8), while the addition of a non-conductive base facbric has little impact on the overall shielding effectiveness.

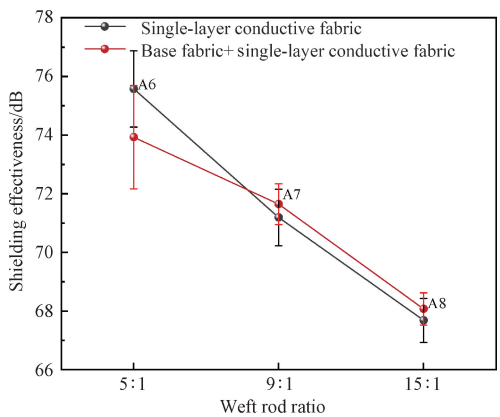

Fig. 6 Shielding effectiveness of fabrics with and without non-conductive base fabric

2.2.6 Influence of number of fabric layers on shielding effectiveness

Fabrics A1, B1 and B6 are selected to investigate the influence of number of fabric layers on shielding effectiveness. As shown in Fig. 7, the shielding effectiveness of a single-layer fabric is lower than that of a double-layer fabric. However, further increasing the number of fabric layers results in a decrease in shielding effectiveness.

The fabrics were made from selected raw materials with consistent conductivity. When two layers were stacked, the shielding effectiveness reached its peak. However, as the number of fabric layers continued to increase, the conductive properties began to decline. This trend occurs because, with a small number of fabric layers, adding more layers introduces additional conductive material into the fabric, thereby enhancing conductivity. However, once the number of layers exceeds a certain threshold, excessive accumulation of conductive material can lead to an uneven distribution within the fabric and a subsequent decline in conductive performance. Additionally, the excessive fabric layers increases internal resistance and capacitance effects, which further destabilize the system and reduce the consistency of the conductive properties. As a result, the shielding effectiveness exhibits a trend of first rising and then gradually declining.

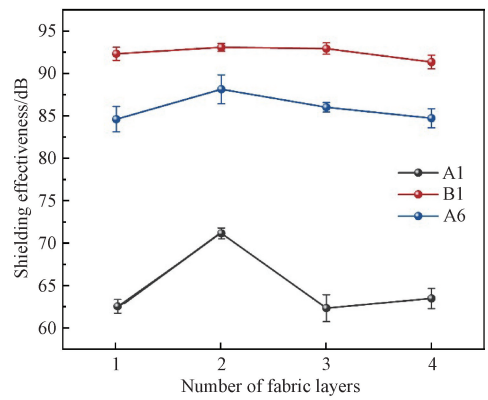

Fig. 7 Curves of shielding effiectiveness vs. number of fabric layers

3 Conclusions

In this study, stainless steel blended yarns, aramid yarns and copper-clad wires were used as raw materials to weave shielding fabrics. The influencing factors and specific trends affecting the shielding effectiveness of the electrostatic field in these fabrics were investigated by varying the fabric weave, yarn type, fabric structure and embedded yarn ratios.

1) When the fabric weave and the content of metal wires in the yarn remain unchanged, an increase in weft

density makes the yarns in the fabric become more compact, increasing the contact points. This reduces the surface specific resistance of the fabrics, enhances conductivity, and improves shielding effectiveness.

2) When the fabric structure remains unchanged and metal fibers are embedded in the fabric, the shielding effectiveness of the bidirectionally embedded one is the highest, then the unidirectionally embedded one, and last the no embedding one. For fabrics with CCWWA embedded only in the weft direction, the addition of CCWWA enhances the shielding effectiveness. Among fabrics with different embedding directions of CCWWA, the bidirectionally embedded configuration provides the best shielding effectiveness, showing an improvement of 8 – 20 dB compared to the fabrics without CCWWA. When CCWWA content per unit area remains constant, arranging CCWWA side by side results in high shielding effectiveness.

3) When the yarn composition and the warp and weft densities of the fabric remain the same, changing the fabric weave results in fabrics with varying shielding effectiveness. The compact structure of the plain fabric provides the best shielding performance, outperforming the basket fabric.

4) The shielding effectiveness of the designed shielding fabric was tested with and without a non-conductive base fabric, and no significant change in the results was observed.

5) Under the same conditions, increasing the number of fabric layers results in the shielding effectiveness increasing first and then decreasing. When the fabric is composed of two layers, the shielding effectiveness of the fabric is the highest.

References

[1] THENKUMARI K, SANKARAN K S, et al. Design and implementation of frequency reconfigurable antenna for Wi-Fi applications [J]. *Engineered Science*, 2023: 876.

[2] WU G F, GAO X G, WAN K F. Mobility control of unmanned aerial vehicle as communication relay to optimize ground-to-air uplinks[J]. *Sensors*, 2020, 20(8): 2332.

[3] JIANG D W, MURUGADOSS V, WANG Y, et al. Electromagnetic interference shielding polymers and nanocomposites: a review [J]. *Polymer Reviews*, 2019, 59(2): 280-337.

[4] SAID S, MELHAOUI O E, GUETBACH Y, et al. Design of a patch antenna for high-gain applications using 1D-EBG structures [J]. *Engineered Science*, 2024, 27: 1040.

[5] WEI C H, HE M K, LI M Q, et al. Hollow Co/NC @ MnO_2 polyhedrons with enhanced synergistic effect for high-efficiency microwave absorption[J]. *Materials Today Physics*, 2023, 36: 101142.

[6] JIA Z X, ZHANG M F, LIU B, et al. Graphene foams for electromagnetic interference shielding: a review [J]. *ACS Applied Nano Materials*, 2020, 3(7): 6140-6155.

[7] FANG F, LI Y Q, XIAO H M, et al. Layer-structured silver nanowire/polyaniline composite film as a high performance X-band EMI shielding material[J]. *Journal of Materials Chemistry C*, 2016, 4(19): 4193-4203.

[8] WANG L, CHENG J W, ZOU Y X, et al. Current advances and future perspectives of MXene-based electromagnetic interference shielding materials [J]. *Advanced Composites and Hybrid Materials*, 2023, 6(5): 172.

[9] ZHENG S N, WU N, LIU Y, et al. Multifunctional flexible, crosslinked composites composed of trashed MXene sediment with high electromagnetic interference shielding performance [J]. *Advanced Composites and Hybrid Materials*, 2023, 6(5): 161.

[10] XUE Y, LIU J H, YANG Z Q. Current status and development trend of individual security protection in power industry[J]. *Cotton Textile Technology*, 2019, 47(9): 74-78. (in Chinese)

[11] XU X L, LI Z, LYU D T, et al. Comparison research on measuring methods for materials shielding effectiveness [J]. *Instrument and Equipments*, 2017, 5(4): 95-105. (in Chinese)

[12] LIU S H, LIU J M, DONG X L. Electromagnetic wave screen dedication and wave-absorbing materials [M]. Beijing: Chemical Industry Press, 2006: 67-71. (in Chinese)

[13] Standardization Administration of the People's Republic of China. Terminology for electromagnetic shielding materials: GB/T 26667—2021[S/OL]. (2021-04-30)[2024-09-01] https://openstd.samr.gov.cn/bzgk/gb/newGbInfo?hcno=F781AC9E998D1E1C5C47CC90A4E90120. (in Chinese)

[14] WANG S. Research on electromagnetic wave absorption based on graphene [D]. Changsha: Hunan University, 2019. (in Chinese)

[15] RONG X. Design and research of high shielding effectiveness multilayer electromagnetic shielding clothing fabric [D]. Zhengzhou: Zhongyuan University of Technology, 2016. (in Chinese)

[16] ZOU Q, SHI C F, LIU B, et al. Enhanced terahertz shielding by adding rare Ag nanoparticles to $Ti_3C_2T_x$ MXene fiber membranes [J]. *Nanotechnology*, 2021, 32(41): 415204.

[17] XU L, LU H H, ZHOU Y, et al. Ultrathin, ultralight, and anisotropic ordered reduced graphene oxide fiber electromagnetic interference

shielding membrane [J]. *Advanced Materials Technologies*, 2021, 6(12): 2100531.
[18] MA J H, ZHAO Q L, ZHOU Y X, et al. Hydrophobic wrapped carbon nanotubes coated cotton fabric for electrical heating and electromagnetic interference shielding [J]. *Polymer Testing*, 2021, 100: 107240.
[19] ZHOU B, LI Z Y, LI Y L, et al. Flexible hydrophobic 2D $Ti_3C_2T_x$-based transparent conductive film with multifunctional self-cleaning, electromagnetic interference shielding and joule heating capacities [J]. *Composites Science and Technology*, 2021, 201: 108531.
[20] LOU C W, LIN T A, CHEN A P, et al. Stainless steel/polyester woven fabrics and copper/polyester woven fabrics: manufacturing techniques and electromagnetic shielding effectiveness[J]. *Journal of Industrial Textiles*, 2016, 46(1): 214-236.
[21] LIU W L, CHEN C H, HAI W Q, et al. Laser-induced graphene conductive fabric decorated with copper nanoparticles for electromagnetic interference shielding application [J]. *Journal of Donghua University (English Edition)*, 2023, 40(6): 571-579.
[22] KRISHNASAMY J, RAMASAMY A, DAS A, et al. Effect of fabric cover and pore area distribution of carbon/stainless steel/polypropylene hybrid yarn-woven fabric on electromagnetic shielding effectiveness [J]. *Journal of Electronic Materials*, 2016, 45(6): 3087-3100.

不锈钢导电织物的制备及其工频屏蔽效能

杨 阳[1], 张 妍[1], 张瑞云[1*], 纪 峰[1], 李文军[2], 徐潇源[3]
1. 东华大学 纺织学院, 上海 201620
2. 杭州赛固迈永盛纺织有限公司, 浙江 杭州 311215
3. 中国棉纺织行业协会, 北京 100027

摘 要: 为制备兼具高效工频屏蔽效能和优良导电性的屏蔽织物, 采用不同比例的芳纶/不锈钢纤维混纺纱织造不同规格的屏蔽织物。对织物的组织结构、面密度、层数、嵌入铜包覆丝比例及方向进行了设计, 共试织 34 种成品织物。通过测试织物电导率及工频屏蔽效能, 研究各种因素对工频屏蔽效能的影响机理。研究结果表明: 屏蔽效能随织物面密度与金属纤维含量的增加而增大; 铜包覆丝的嵌入, 特别是双向嵌入, 使织物屏蔽效能得到极大改善, 相较于无嵌入铜包覆丝织物, 嵌入铜包覆丝织物的屏蔽效能提高 8~20 dB; 不同结构机织物得到的屏蔽效能不同, 平纹织物因其结构紧密, 屏蔽效能较大; 非导电基布对织物屏蔽效能影响不大; 随织物层数增加屏蔽效能先增大后减小, 双层织物的屏蔽效能最大。

关键词: 不锈钢混纺织物; 工频; 屏蔽效能; 导电性; 安全防护